Current Science
CS 6 (4), 6438-6453 (2026)
Received 12 June 2026 | **Accepted 27 June** 2026 | **Online Available 04 July** 2026
https://doi.org/10.52845/CS/2026-6-4-4

Current Science

Current Science

OPEN ACCESS

ISSN(O)2795-8639

Original Article

Research on Surface Structure Optimization and Water Film Phase Change of Plate-Tube Evaporative Condenser

Xiang-yun Liu[1,2*], Kai Sun[2], Liangde Liu[2], Xiufang Ke[2], Guansheng Chen[2], Chao Wei[1*]

[1]School of Intelligent Engineering, Guangzhou Songtian Polytechnic College, 511370, China

[2]School of Material and Energy, Guangdong University of Technology, China, 510006

***Corresponding Author: Xiang-yun Liu, Chao Wei**

Abstract:
To investigate the flow and heat transfer characteristics of a plate-fin evaporative condenser and to optimize its internal cavity structure, this study employs a combination of experimental methods and numerical simulations based on the commercial software Fluent. A mathematical model describing the gas-liquid two-phase flow is established, and the heat transfer performance of the heat exchanger is thoroughly examined. By comparing the experimental results with the simulation outcomes, good agreement is found in key parameters, which validates the accuracy and reliability of the numerical model. Based on this, the study analyzes the variation of the Nusselt number on the plate surface and the distribution characteristics of the water film under different Reynolds numbers. Consequently, the optimal cavity depth is determined to be H=2.0, and the optimal small diameter is D1=6mm. Under these optimal structural conditions, the influence of ten different inlet Reynolds numbers (ranging from 3500 to 13500) on the water film thickness is further investigated. The results indicate that as the Reynolds number increases, the water film thickness initially increases and then gradually tends to stabilize; that is, once the Reynolds number reaches a certain value, the growth rate of the water film thickness slows down significantly and approaches a constant value.

Key words: water film,enhanced heat transfer,structural optimization,gas-liquid two-phase

Introduction

Evaporative condenser is an efficient, energy-saving and water-saving equipment with low energy consumption in industry. It combines the heat exchanger and cooling tower together in the structure, which not only has a compact structure but also has low operating costs [1-4]. It is widely used in multiple industrial fields [5,6].

A large amount of scientific research has been conducted both domestically and internationally on the performance of evaporative condensers. Xie Yingchun et al. used numerical methods to study the characteristics of vertical tube evaporation and condensation[7]. The falling film inside the tube was divided into an initial section, a stable section, an undulating section, and a fluctuating section. The disturbance of the reverse airflow would change the distribution position and range of the four parts inside the tube. The thickness of the liquid film also depends on the size of the Reynolds number. If it is too large, it will cause dry wall phenomenon, and if it is too small, it will make the liquid film thinner and weaken the anti-interference ability. Dai Yadong et al. [8] used numerical simulation methods and adopted the VOF model to study the influence of tube shape, fin spacing, longitudinal tube rows, and frontal wind speed on the heat transfer performance of finned tube evaporative condensers. Lee [9] conducted experimental and simulation studies on the heat transfer performance of spray falling film on horizontal

tubes, and compared the liquid film distribution characteristics and heat transfer coefficient distribution of the upper and lower tubes under different spray flow rates, different spray angles, different horizontal tube spacing, and wind direction upstream and downstream. Zhu [10] discussed in detail the effects of important parameters such as spray density, face velocity, ambient temperature, and humidity on heat and mass transfer performance, and found that wet bulb temperature has a greater impact on heat transfer performance than relative humidity. Corrugated plate or tubes were also used to simulate the evaporative effect of spray water [11-13]. However, due to the advantages of lighter weight, smaller volume, wider heat transfer surface, and higher heat transfer efficiency compared to tube types [14], research on plate types has gradually increased in recent years. Yuan Hong conducted a study on the enhanced heat transfer of plate heat exchanger with different pump pulsation intensities[15]. Yang Jun et al. used numerical simulation methods to investigate the effects of straight and Z-channels on the heat transfer flow characteristics of printed circuit plate heat exchangers[16]. Jiang Xuejing et al. studied the influence of different parameter combinations on the comprehensive evaluation coefficient of corrugated spiral plate heat exchangers and found that the influence of wave height was greater than that of other parameters[17]. Wang et al. used genetic algorithm to perform double-layer multi-objective optimization on the different structural sizes of concave holes in convex plate heat exchanger. Experiments and numerical simulations was also conducted on the heat transfer and flow characteristics on convex plates[18]. However, there have been rare reports about the detailed influence of plate tube evaporative condenser on the liquid film. This paper uses a combination of numerical simulation and experimental methods to study the influence of different sizes of recessed holes in plate and tube evaporative condenser.

1. Models

1.1 Geometric Model

The experimental setup is shown in Fig.1, which is mainly composed of standard refrigeration cycle components and an evaporative condensing chiller unit. Figure 2 shows the experimental setup of an evaporative condenser designed based on simulation optimization of the structure. Heat exchange occurs between the refrigerant inside the plate and tube evaporative condenser through the evaporation flow of spray water and air. Figure 3 shows the geometric model of a single plate of the plate and tube heat exchanger used in the plate and tube evaporative condenser. Its external dimensions are length x width x height=309mm x 2mm x 774mm, with regularly distributed concave holes on the surface, which increase the contact area and enhance turbulence.

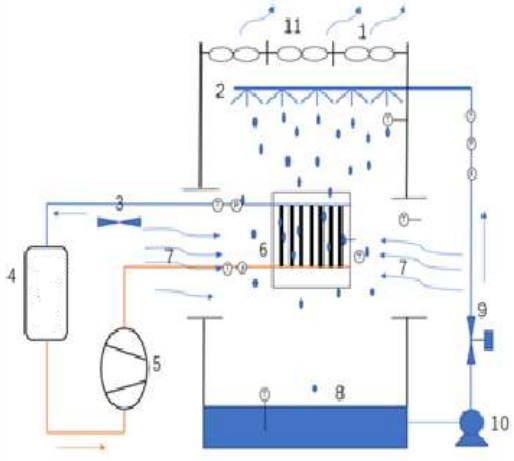

Fig. 1 Experimental Setup

1. Fan, 2. Spray water, 3. Throttle valve, 4. Evaporator, 5. Compressor, 6. Heat exchanger **plate, 7. Air inlet, 8. Water tank, 9. Three way valve, 10. Water pump, 11. Air outlet, T-Temperature measuring point, F-Flow measuring point**

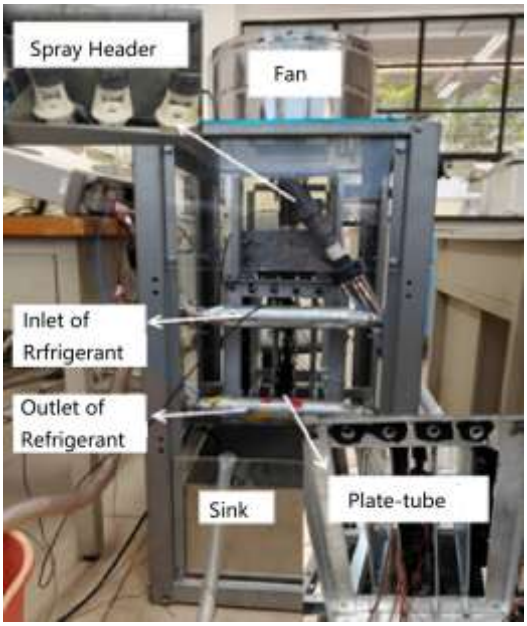

Fig 2. Test device of plate tube evaporative condenser

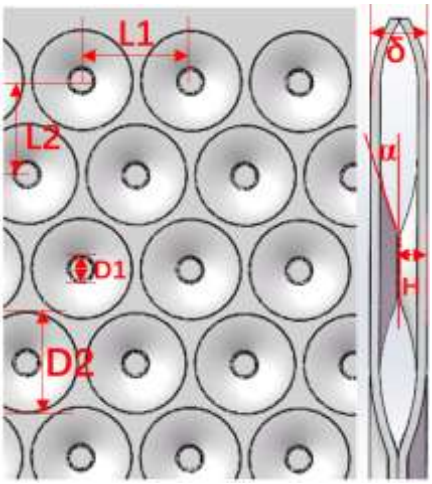

***L*$_1$=*L*$_2$=26mm,*D*$_1$=2～12mm(8 sizes),*D*$_2$=24mm,*δ*=4mm,*H*=1~3mm(9个尺寸)**

Fig 3. Front view of the Plate

1.2 Control Equations

1.2.1 Continuity Equation[18]:

$$\frac{\partial}{\partial t}(\rho)+\nabla\cdot(\rho\vec{u})=0 \quad (1)$$

1.2.2 Momentum conservation equation[18]:

$$\frac{\partial}{\partial t}(\rho\vec{u})+\nabla\cdot(\rho\vec{u}\vec{u})=-\nabla P+\nabla\cdot\left[\mu\left(\nabla\vec{u}+\vec{u}\right)\right]+\rho\vec{g}+\vec{F} \quad (2)$$

Where, $\vec{F}$ is the momentum source term, which is the sum of surface tension and shear force at the gas-liquid interface.

1.2.3 Energy conservation equation:

$$\frac{\partial(\rho E)}{\partial t}+\nabla\cdot(\vec{v}(\rho E+p))=\nabla\cdot\left(k_{\text{eff}}\nabla T\right)+S_{\text{h}} \quad (3)$$

$$S_h = h_{wf} S \quad (4)$$

Where,S is the energy source term, and h_{LW} is the latent heat of vaporization of the water film.

1.2.4 Mass transfer equation[19] :

$$\frac{\partial \alpha_j \rho_j \omega_j^k}{\partial t} + \nabla \cdot (\alpha_j \rho_j \vec{u} \omega_j^k - \alpha_j \varphi_j \nabla \omega_j^k) = S_{wf}^k \quad (5)$$

$$k = 1,2,...,r \quad (6)$$

where， ω_j^k represents the mass fraction of the k-th component in the j-phase, $S_{wf}^k$is the mass transfer source term of the water film， φ_j is the mass transfer diffusion coefficient.

1.2.5 Volume fraction(VOF) equation:

By using the VOF method to track and calculate the volume fraction distribution within a unit, the position of the phase interface can be determined. The distribution of the interface is represented as:

$$\frac{\partial \gamma_i}{\partial t} + \vec{u} \cdot \nabla \gamma_i = 0 \quad (8)$$

$$\sum_{i=L,G} \gamma_i = 1 \quad (9)$$

where, γ_i is the volume fraction within the calculation unit. When γ_i=0, indicates that there is no phase i in the unit ; when γ_i=i, indicates that the unit is entirely composed of phase i ; when0<γ_i<1, indicates that ther is an interface between the i-th phase and other phases in this unit[20].

Where the ρ and μ can be expressed as follows ：

$$\rho = \gamma_l \rho_l + (1-\gamma_l)\rho_g \quad (10)$$

$$\mu = \gamma_l \mu_l + (1-\gamma_l)\mu_g \quad (11)$$

1.3 Boundary Condition

The fluid part between two adjacent plate walls of the condenser is taken as the calculation domain. According to reference[21], the thermal resistance of the plate tube evaporative condenser mainly occurs on the water and air sides. Therefore, it is idealized as a gas-liquid two-phase flow process on an infinitely large vertical plate.As shown in Figure 4, due to the symmetric structure of the model, half of the fluid domain between the two plates is modeled using symmetric boundary conditions. Adopting the standard k - ε model and two-phase flow VOF model, the two-phase application of moist air and water component transport model. The water side temperature is set to 305.5K, the inlet Reynolds number is 7500, the air side inlet temperature is 303.66K, the velocity is 2m/s, and the relative humidity is 74%. Based on experience, a constant heat flux density of q=4000W/m2 is used as the refrigerant side condition.

The Reynolds number at the inlet and the average Nusselt number of the plate and tube are defined as follows:

$$\mathrm{Re} = \frac{ud}{\nu} \quad (12)$$

$$Nu = \frac{hd}{\lambda} \quad (13)$$

where, u is inlet speed of water film, d is equivalent diameter of water film inlet, h is the heat transfer coefficient between water film and air, it can be defined as follows :

$$\begin{cases} h = \left[h(X_1) + h(X_2) + \ldots + h(X_n)\right]/n \\ h(X_i) = q/\left[T_w(X_i) - T_a(X_i)\right], i = 1,2,...,n \end{cases} \quad (14)$$

Where, X_i represents different cross-sections in the z-direction, $T_w(X_i)$ is the average temperature of the water film at that cross-section, and $T_a(X_i)$ is the average temperature of the air at that cross-section.

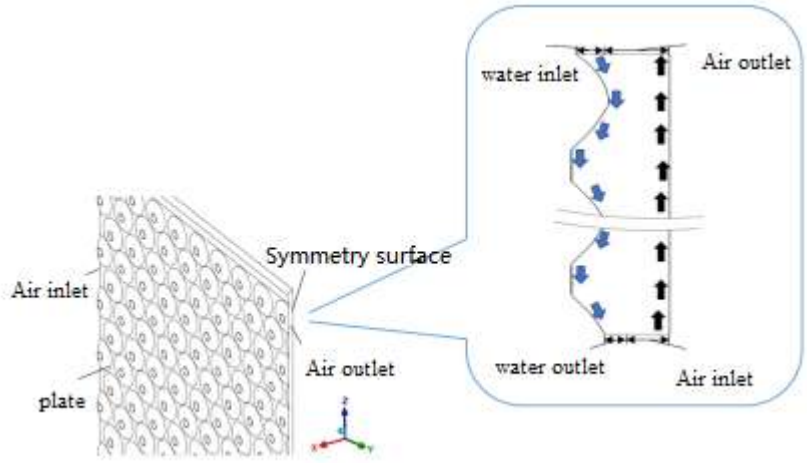

Fig.4 Diagram of computational domain model and boundary conditions

1.4 Grid Independence Verification

In order to balance the accuracy and computational efficiency of the grid, independence verification was performed on the generated 9 sets of grids with increasing numbers. The geometric model was adopted with a concave structure size of D1=6mm and H=2mm. The model mesh adopts a hexahedral unstructured mesh, and wall function was applied in the concave area.

Figure 5 shows the variation of the mass fraction of water vapor(ω_{air}) at the air outlet and the average temperature(T_{av}) of the plate with the number of grids. As the number of grids increases from 264955 to 1056913, ω_{air} shows an increasing trend, while T_{av} first decreases and then increases. After the number of grids reaches 1391668, ω_{air} and T_{av} begin to stabilize, with respective numerical changes not exceeding 0.0005 and 0.002K. Therefore, this paper adopts the minimum number of grids when the parameters are stable, which is 1391668.

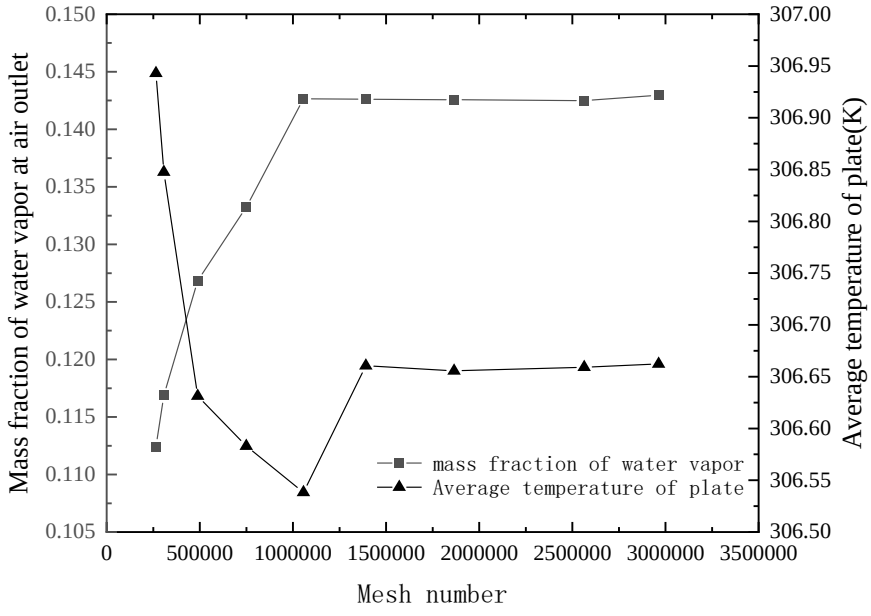

Fig. Mass fraction of water vapor at the air outlet and average temperature of the plate under different grid numbers

2. Numerical simulation

2.1 Optimization analysis of plate concave depth (H)

The structure of the plate directly affects the wetting coverage and natural evaporation effect. This article analyzes the variation of the depth H and small diameter D1 of the concave holes in the plate to indicate the flow and heat transfer characteristics.Table 1 lists the dimensions of the concave holes at different depths, with only the height H changing and D2=2mm.

Table 1 Different Depth H Dimensions of Concave Holes (D1=2mm)

Depth	*H1*	*H2*	*H3*	*H4*	*H5*	*H6*	*H7*	*H8*	*H9*
unit(mm)	1.00	1.25	1.50	1.75	2.00	2.25	2.50	2.75	3.00

Figure 6 shows the effect of H on Nusselt number at different Reynolds numbers. There are six operating conditions with Reynolds numbers ranging from 7500 to 17500. It can be seen that for all Reynolds number conditions, when H increases from 1.0mm to 1.5mm, the increase in Nusselt number is significant, and the change in Nusselt number is small when H increases from 1.5mm to 2.0mm. After H=2.0mm, the Nusselt number gradually decreases with the increase of H. This indicates that the plate heat transfer effect is best when H=2.0mm.

Figure 7 shows the distribution of water film at H=2.0mm. It can be seen that at Re=7500, the area where the volume fraction of water on the plate is lower than 0.5 is larger, which means that the dry spot area is larger, and the dry spot areas are almost concentrated at the same height a. This phenomenon is due to the fact that when the water film falls from the top of the plate to point a, most of its kinetic energy is consumed, causing most of the water flow to flow into the raised part of the plate with greater curvature, resulting in dry spots appearing in the surrounding flat areas of the plate. When the Reynolds number increases, the water flow can obtain greater kinetic energy when passing through the same position. When Re reaches 13500, the dry spot area at position a begins to significantly decrease.

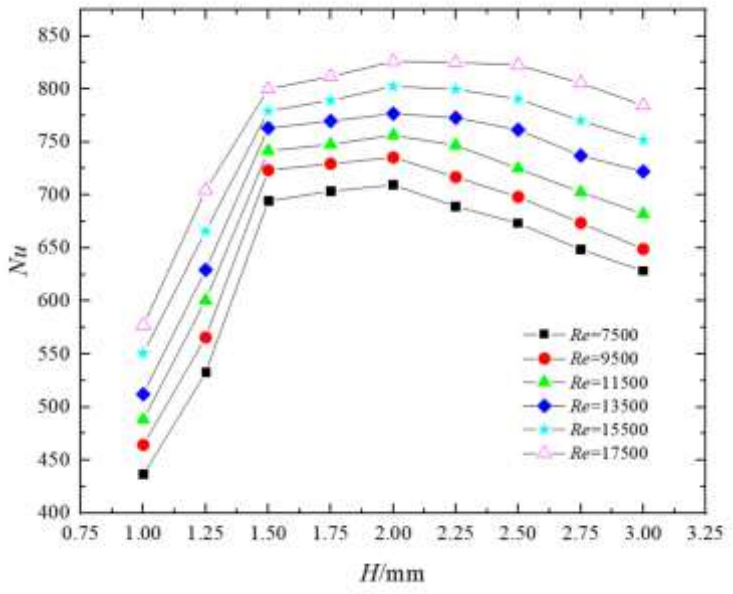

Fig.6 Effect of H on Nusselt numbers at different Reynolds numbers

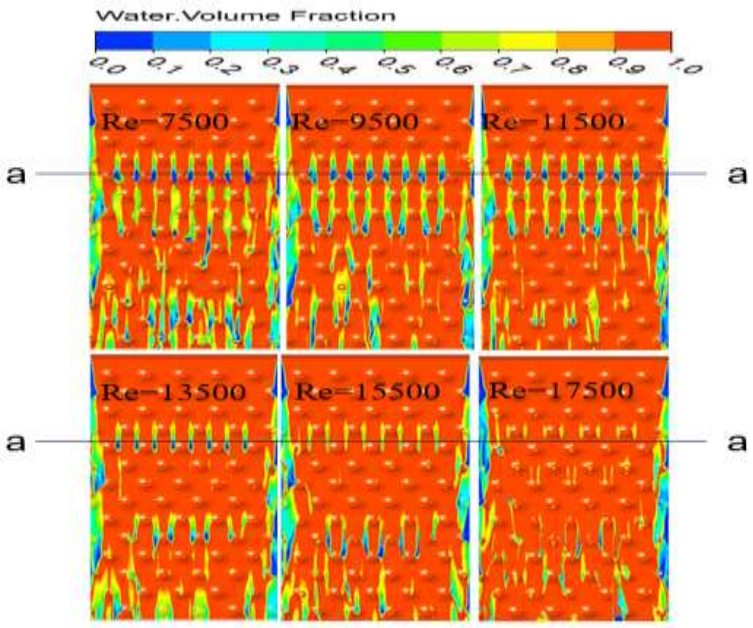

Figure 7: Volume fraction of water film on plates at different Reynolds numbers (H=2.0mm)

Figure 8, it can be seen that as H increases, the dry spot area on the plate increases. This is because the inclination angle α at the concave part of the plate is too large, causing more water to flow into the concave part of the plate. However, at this time, the water flow rate is limited, which leads to a decrease in the liquid film on the flat part of the plate on the same horizontal line b as shown in I when H=3mm, and even excessive dry areas appear, resulting in weakened heat transfer; At the same time, a large number of dry spots also appeared in the depression of the plate at the lower height II. This is because as H increases, the inclined surface area of the concave holes in the plate also increases, and the lower height is also the area where the water flow obtains greater kinetic energy in the direction of gravity. At this time, less water flow will completely pass through the entire inclined area, resulting in many dry spots. It is obvious that when H is greater than 2mm, due to the small water flow rate and the increase in tilt angle α, a large number of dry spots appear. At this time, the heat transfer weakening effect caused by dry spots will be stronger than the heat transfer strengthening effect. Therefore, H=2mm is actually the critical value for the occurrence of a large amount of dry spots.

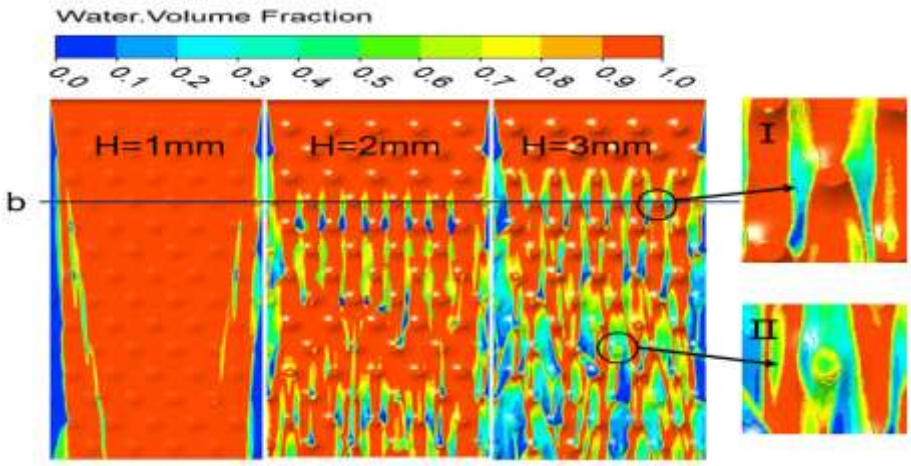

Fig.8 Distribution of water volume fraction with three different *H*

The distribution of water film thickness under different Reynolds number conditions is shown in Figure 9. It can be seen that the water film thickness gradually increases with the increase of Re, from 1.9mm to 2.6mm, and the growth rate slows down after Re reaches 15500. This is because water is subject to gravity, which prevents the water film thickness from increasing infinitely in the horizontal direction.

Figure 10 shows the curve of the water film pressure drop on the surface of the plate as a function of Re, and it can be clearly observed that the pressure drop increases continuously. When Re increased from 7500 to 17500, the pressure drop increased from 13.93 to 30.14, with an increase of 29.6%. This is because the higher the Reynolds number, the higher the turbulence level of the liquid film flow, and the greater the shear force between it and the air, resulting in an increase in the kinetic energy loss of the water film.

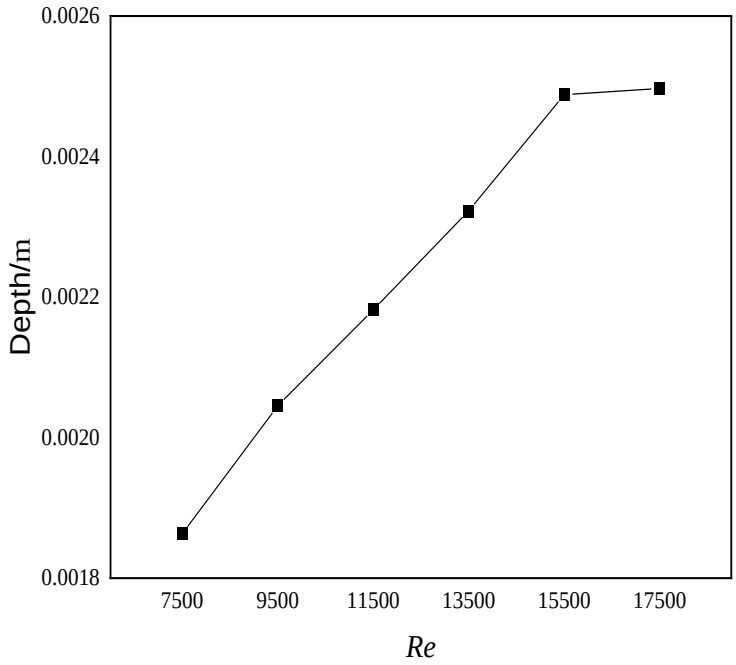

Fig.9 The average thickness of the water film at different Reynolds numbers (H=2mm)

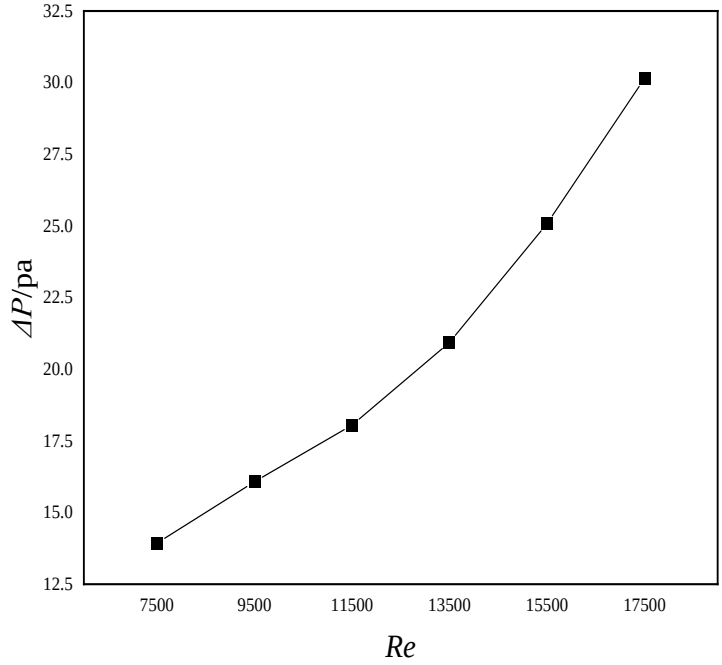

Fig.10 Water film pressure drop variation at different Reynolds numbers (H=2mm)

2.2 The influence of small diameter D1 of concave holes on flow and heat transfer

In the case of optimizing the height of the concave hole H on the above-mentioned board, a comparative study was conducted on the influence of eight sizes of the small diameter D1 of the concave hole from 2-12mm when H=2mm was selected. Figure 11 shows the variation of Nusselt number (Nu) with D1 under different Reynolds number (Re) conditions. It can be seen that as D1 increases, the Nusselt number (Nu) also shows a trend of first increasing and then decreasing. Under the condition of Re=7500, when 2mm<D1<6mm, Nu increased from 8.03 to 8.47. But when 6mm<D1<12mm, Nu began to continuously decrease, dropping from 8.47 to 5.98.

Under the optimization of H height mentioned above, H=2mm was selected to compare and analyze the small diameter D1 of the recessed hole from 8 scales of 2-12mm. Figure 11 shows the variation of Nusselt number (Nu) with D1 under different Re values. As D1 increases, Nu also shows a trend of first increasing and then decreasing. Under the condition of Re=7500, when 2mm<D1<6mm, Nu increased from 8.03 to 8.47. When 6mm<D1<12mm, Nu began to continuously decrease from 8.47 to 5.98.

Under the optimization of H height mentioned above, H=2mm was selected to compare and analyze the small diameter D1 of the recessed hole from 8 scales of 2-12mm. Figure 11 shows the variation of Nusselt number (Nu) with D1 under different Re values. As D1 increases, Nu also shows a trend of first increasing and then decreasing. Under the condition of Re=7500, when 2mm<D1<6mm, Nu increased from 8.03 to 8.47. When 6mm<D1<12mm, Nusselt number began to continuously decrease from 8.47 to 5.98.

Compared to Figure 12, during the process of D1 increasing from 2mm to 6mm, although several dry spots appeared, Nu did not decrease but instead increased. This is because the increase of D1 leads to an increase in the heat transfer area of the plate, while also making the air flow channel wider, resulting in more drastic changes in the velocity and direction of air flow, which is conducive to the diffusion of high-temperature and high humidity air near the wall, thereby promoting gas-liquid heat and mass exchange. At

this time, the heat transfer enhancement effect is greater than the weakening effect of dry spots. For cases where D1 is greater than 6mm up to 12mm, the dry spot area begins to increase significantly, as the continuous growth of D1, like the growth of H, actually leads to an increase in area and tilt angle α. It can be seen that when D1=12mm, the small diameter top in the local magnified image has a relatively large inclination angle α, resulting in less water flowing in and a lower water mass fraction. And due to the fact that the increase in D1 has a greater impact on the growth of the plate area, its influence is stronger than that of the increase in H on the plate area. At a small flow rate of Re=7500, due to the low spray flow rate, large areas of dry areas appear on both sides of the plate, as shown in II. When the enhanced heat transfer caused by the increase in heat transfer area cannot offset the heat transfer deterioration caused by the increase in dry spots, Nu begins to decrease.

Figure 13 shows the changes in air pressure drop under different D1 values at Re=7500. It can be observed that the difference between the maximum and minimum values of pressure drop does not exceed 0.2pa during the process of D1 changing from 2mm to 12mm. Therefore, it can be considered that within this range, the change in D1 size has almost no effect on the change in pressure loss.

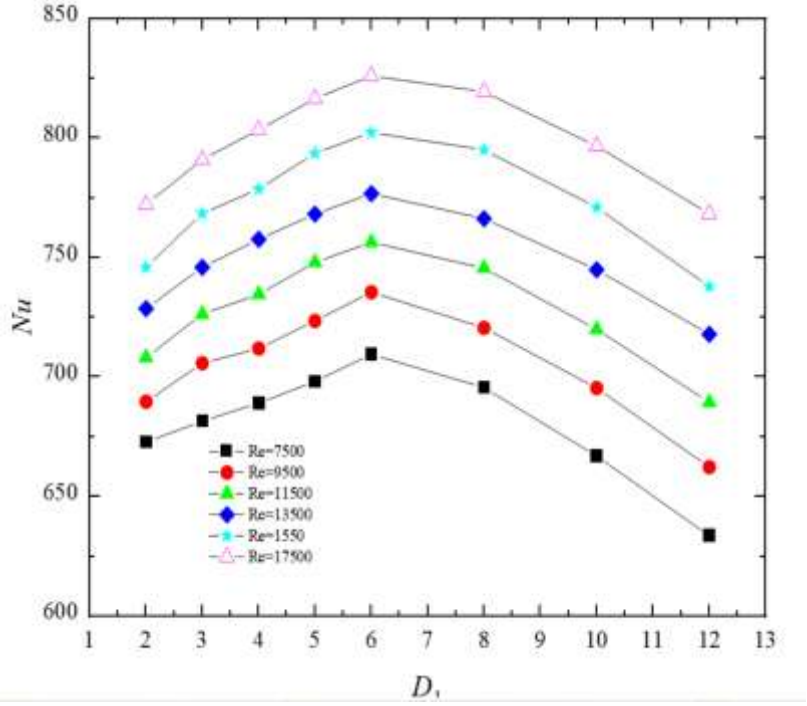

Fig.11 Variation of Nu with D1 under different Re

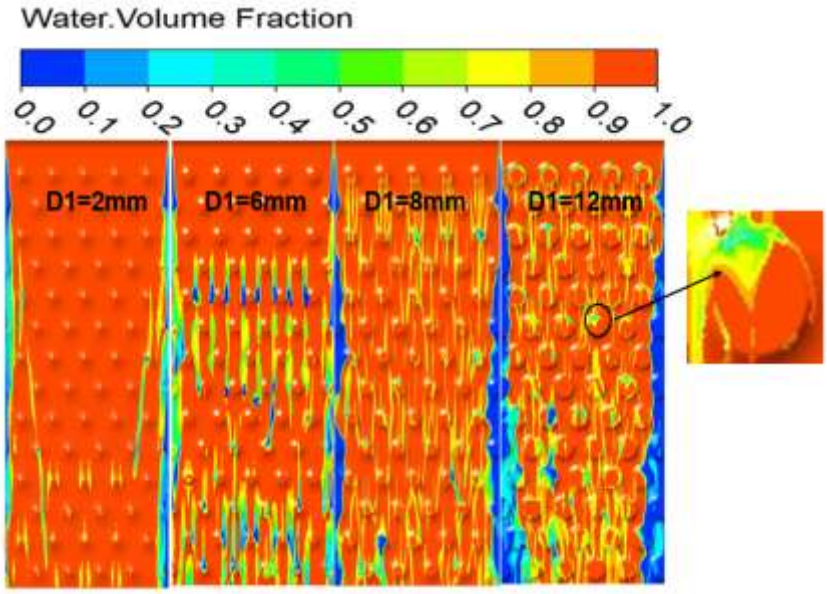

Fig.12 Distribution of liquid film on three different D1 plates at Re=7500

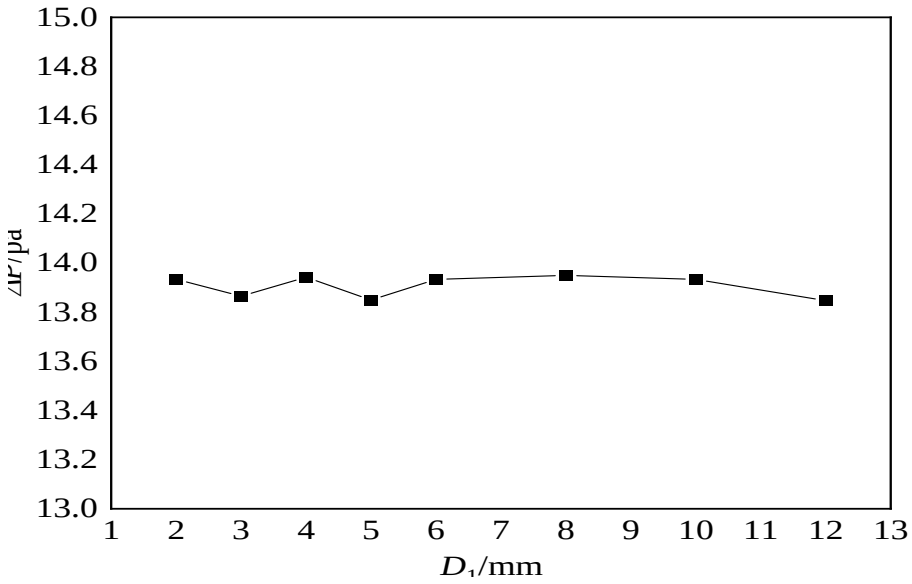

Fig. 13 Distribution of air pressure drop at different D1 when Re=7500

The heat transfer intensity of the plate will increase with the increase of Re, but the pressure drop of the air is also constantly increasing, which is a serious problem for the power consumption of water pumps and fans. Therefore, in fact, the heat transfer effect does not improve with the increase of Re. It is necessary to comprehensively consider the cost and efficiency in actual industrial production in order to determine the optimal working parameters.

2.3 The influence of different Reynolds numbers at water inlet

Keeping the parameters of the optimal model, including its structure (H=2mm, D1=6mm), wind speed, and air moisture content, constant, an investigation was conducted on ten operating conditions on the water side, corresponding to Reynolds numbers (Re) of 3500, 4800, 5800, 6800, 8000, 9000, 10000, 11000, 12000, and 13500. As illustrated in Figure 14, with the gradual increase of Re from 3500 to 13500, the rising flow rate enhances the disturbance of the

water flow against the plate surface. This leads to a continuous increase in water velocity and a gradual rise in the water volume fraction at the edges on both sides of the plate surface, indicating a progressive reduction of dead zones, as shown in Figure 15. Concurrently, as depicted **in Figure 16, the thickness of the water film on the plate surface gradually increases with the rise in Re, growing from 1.87 m to 2.52 m. However, after Reynolds number reaches 9000, the growth rate slows down significantly and approaches a constant value. This occurs because the water film thickness cannot increase indefinitely in the horizontal direction due to the effect of gravity.**

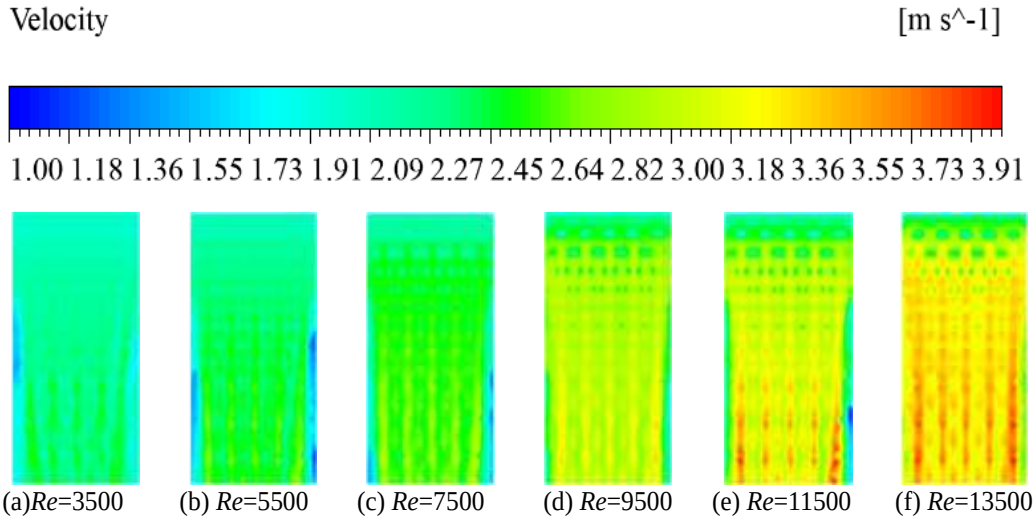

Fig.14 Velocity distribution contour of gas-liquid mixture at x=0.25m section for different Re

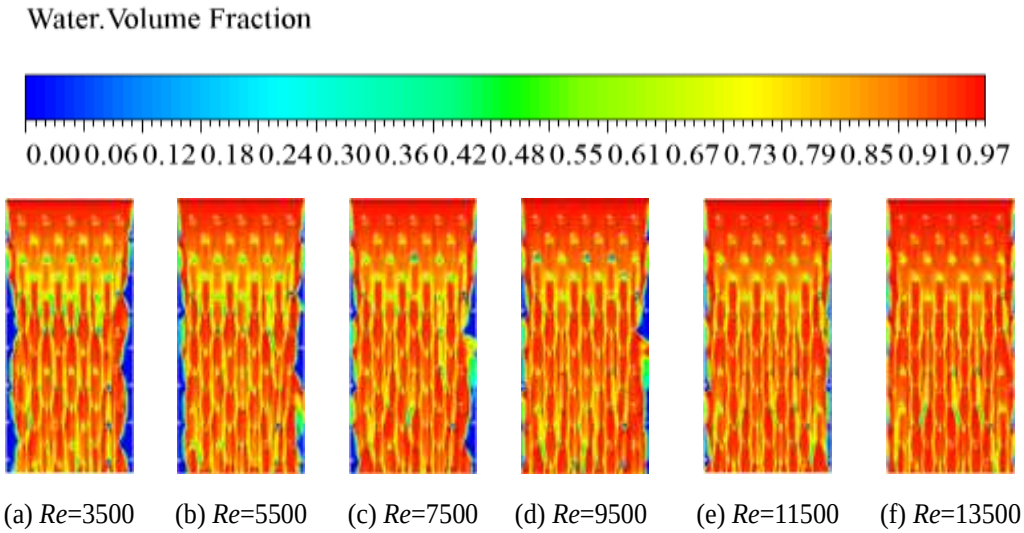

Fig.15 Water volume fraction distribution contour on the surface of the plate for different *Re*

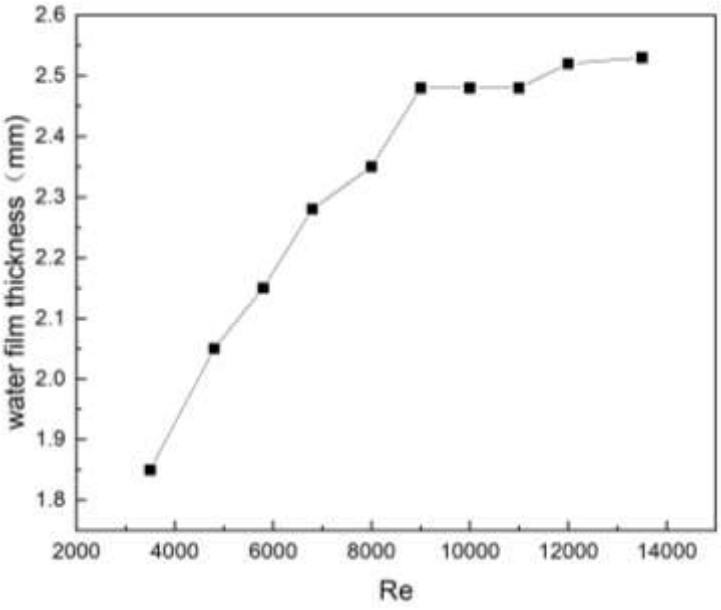

Fig.16 Variation of average water film thickness with increasing Re

2.4 Comparison of Experimental and Simulation Results

Based on the optimal size of the recessed hole obtained from the above simulation (H=2mm, D1=6mm), experimental specimens were designed, and the experimental setup diagram is shown in Figure 3 above. The experiment used an Agilent 34972a data collector to collect temperature data from various locations on the device through thermal-couples. The LZS-15 rotor flow-meter was used to measure the water flow rate flowing out of the spray nozzle. An anemometer and a temperature and humidity meter were used to measure the velocity, temperature, and humidity of the inlet and outlet air of the evaporative condenser.

Figure 17 compares the experimental and simulated data of Nu measured under different Re values. It can be seen from the figure that the trend of the simulated and experimental values is the same, and the error does not exceed 5%, which proves the reliability of the numerical simulation method of the model.

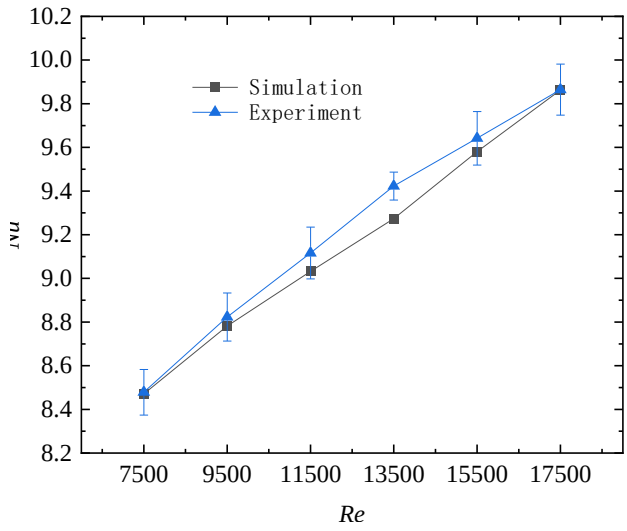

Fig.17 Comparison of Nu under Different Re Experiments and Simulations

Conclusion

This article conducted experimental and numerical simulation analysis on the fluid domain outside a single plate of an evaporative condenser, studied the effects of different gas-liquid conditions and concave structures on flow and heat transfer characteristics, and obtained the following main conclusions:

1) The experimental results are in good agreement with the numerical simulation results.
2) Under all Reynolds number conditions, as the depression height of the plate increases, Nu shows a trend of first increasing and then decreasing, and the plate height H=2.0 is the optimal depression height size.
3) The thickness of the liquid film covering the surface of the plate increases with the increase of Re, and the pressure drop of the liquid film increases with the increase of Reynolds number.
4) Under all Reynolds number conditions, as the concave diameter of the plate increases, Nusselt number shows a trend of first increasing and then decreasing, corresponding to a critical value of 6.0mm for the small diameter of the plate.
5) The height of the plate depression has a significant impact on the pressure drop with air, while the small diameter D1 of the plate depression has little effect on the pressure drop with air.

Research has shown that under the premise of ensuring sufficient water flow rate and good wetting effect of the plate, the area and inclination angle of the concave structure will be better when they are at appropriate angles (i.e., when H and D1 are optimal), resulting in better heat transfer effect. However, the higher the Reynolds number, the higher the energy consumption. Therefore, in actual industrial production, it is necessary to balance energy consumption and heat transfer efficiency, fully considering both factors.

Acknowledgment:

This paper are supported by Guangzhou Science and Technology Plan 2025: Special Topic on the Construction of Industry Science and Technology Collaborative Innovation Centers(No. 2025B04J0010/2025B04J0008) ,the Science and Technology Innovation Bureau of Zengcheng Economic and Technological Development Zone(2024ZCKJ25),2023 Special Innovation Project for Universities in Guangdong Province (GSZKHT2023C009).

Symbols:

C_P——*specific heat capacity at constant pressure,J/(kg·K)*

D1——Small diameter of cavity,*mm*

$\vec{F}$ ——The momentum source term,N

H——Depth of cavity,*mm*

h——Coefficient between water film and air,$W/(m^2.K)$

ΔP——Pressure Drop,*Pa*

T——Temperature,*K*

Re——Renold Number($\mathrm{Re}=\frac{ud}{\nu}$)

α——Angle between cavity and plumb line,*Deg*

q——Heat flux density,W/m^2

E——*internal energy,J*

K——*heat transfer coefficient,W/(m·K)*

k——*turbulence kinetic energy*

u——*velocity in the x-axis direction,m/s*

v——*velocity in the y-axis direction,m/s*

w——*velocity in the z-axis direction,m/s*

M——*molecular weight,g/mol*

p——*pressure,Pa*

R——*gas constant*

r——*reaction rate,m3/s*

S——*resource item*

t——*time,s*

T——*temperature, K*

V0——*Theoretical air volume,m3*

V——*Actual air volume,m3*

Nu——Nusselt number($Nu = \frac{hd}{\lambda}$)

Symbols:

ρ——*decity,kg/m*^{3}

ε——*turbulent dissipation rate*

σ——*unit shearing stress,Pa·s*

μ——*dynamic viscosity,Pa·s*

Subscript:

air——*air phase*

p——*constant pressure*

wf——*water film*

x——*x axis*

y——*y axis*

z——*z axis*

i—— substance i

j—— substance j

Conflict of Interest Statement：

The authors declare that there are no conflicts of interest regarding the publication of this article. No financial or non-financial interests, relationships, or affiliations have influenced the design of the study, the collection, analysis, and interpretation of data, or the writing of this manuscript. All authors have read and approved the final version of the manuscript and confirm that there is no competing interest to disclose.

Reference

1. Liu Dexing Application of Evaporative Condenser in Refrigeration System [J]. Shanghai Energy Conservation, 2007 (4): 35-36.
2. Guo Shengjiang, Chen Guobang, Dong Xingjie Feasibility Analysis of Evaporative Condenser Used in Cooling System of Thermal Power Plant [J/OL]. Energy Engineering, 2004 (4): 53-57. DOI: 10.16189/j.cnki-nygc.2004.04.014.
3. Wu Zhijiang, Wang Nan, Zhu Dongsheng Experimental Study on Enhanced Heat Transfer of Vertical Evaporative Condenser [J]. Low Temperature Engineering, 2010 (03): 26-29+60.
4. Zhang Xu, Tu Shuping, Sun Wenzhe Research and Application Progress of Evaporative Condensers [J/OL].Applied Chemistry,2019,48(5):1178-1180+1185.DOI: 10.16581/j.cnki.issn1671-3206.20190311.011.
5. Wu Xiaowei, Zhao Xun, Chen Zuming, etc Analysis of the Impact of Heat Recovery on Water Cooled Chillers [J]. Energy saving Technology, 2023, 41 (2): 165-170.
6. Zhou Xiangjiang, Lian Zhiwei, Liu Hongmin, etc Feasibility analysis of using water-cooled units for year-round air conditioning [J]. Energy saving technology, 2003 (1): 3-4+10.
7. Xie Yingchun, Liu Jun, Xu Chang, etc Study on the Flow Characteristics of Liquid Film in Vertical Falling Film Evaporation Condensation Tube [J]. Fluid Machinery, 2022, 50 (06): 39-46.
8. Dai Yadong, Sun Hong, Feng Wei, etc Research on Heat Transfer Characteristics and Structural Optimization of Finned Tube Evaporative Condenser [J]. Energy saving Technology, 2023, 41 (5): 400-407419.
9. LEE Y T, WEN C Y, CHIEN L H, etc. Heat transfer of spray falling films over horizontal tubes with counter current airflows in an evaporative condenser[J/OL]. International

Journal of Heat and Mass Transfer, 2022, 183: 122199. DOI:10.1016/j.ijheatmasstransfer.2021.122199.

10. ZHU X, CHEN S, SHEN S, etc. Experimental study on the heat and mass transfer characteristics of air-water two-phase flow in an evaporative condenser with a horizontal elliptical tube bundle[J/OL]. Applied Thermal Engineering, 2020, 168: 114825. DOI:10.1016/j.applthermaleng.2019.114825.
11. Sun Fengdan Numerical simulation of fluid flow characteristics on corrugated plate surface [J/OL]. Modern Chemical Engineering, 2012, 32 (1): 90-93. DOI: 10.16606/j.cnki. issn0253-4320.2012.007
12. KACHHWAHA S S, DHAR P L, KALE S R. Experimental studies and Numerical simulation of evaporative cooling of air with a water sprayII. Horizontal counter flow[J/OL]. International Journal of Heat and Mass Transfer, 1998, 41(2): 465-474. DOI:10.1016/S0017-9310(97)00131-2.
13. Jiang Xiang, Zhu Dongsheng, Tang Guangdong Research on the Heat Transfer Performance and Mechanism of Water Film and Air Outside Evaporative Condenser Tubes [J]. Fluid Machinery, 2006 (8): 59-62
14. ABU-KHADER M M. Plate heat exchangers: Recent advances[J/OL]. Renewable and Sustainable Energy Reviews, 2012, 16(4): 1883-1891. DOI:10.1016/j.rser.2012.01.009.
15. Yuan Hong, Ding Yuxin, Li Rui Experimental study on pulsating flow enhanced heat transfer based on marine plate heat exchangers [J]. Energy saving Technology, 2017, 35 (5): 433-437.
16. Yang Jun, Liu Huanpeng Numerical Analysis of Heat Transfer Flow Characteristics of Printed Circuit Plate Heat Exchanger [J]. Energy saving Technology, 2023, 41 (3): 273-278+283.
17. Jiang Xuejing, Liu Jiao, Ye Zhiqiang, etc Research on Heat Transfer Performance of Corrugated Spiral Plate Heat Exchanger [J]. Energy saving Technology, 2023, 41 (4): 372-378.
18. WANG D, ZHANG H, WANG G, et al. Experimental and Numerical study on the heat transfer and flow characteristics of convex plate heat exchanger based on multi-objective optimization[J/OL]. International Journal of Heat and Mass Transfer, 2023, 202: 123755. DOI:10.1016/j.ijheatmasstransfer.2022.123755.
19. Gu Fang, Liu Chunjiang, Yu Liming, etc CFD study on gas-liquid two-phase falling film flow and mass transfer process [J]. Journal of Chemical Engineering, 2005 (04): 438-444.
20. HIRT C W, NICHOLS B D. Volume of fluid (VOF) method for the dynamics of free boundaries[J/OL]. Journal of Computational Physics, 1981,39(1): 201-225. DOI:10.1016/0021-9991(81)90145-5.
21. PEREZ-BLANCO H, BIRD W A. Study of Heat and Mass Transfer in a Vertical-Tube Evaporative Cooler[J/OL]. Journal of Heat Transfer, 1984,106(1):210-215. DOI:10.1115/1.3246637.